AD NUMBER
AD010029
CLASSIFICATION CHANGES

TO:	unclassified
FROM:	confidential

LIMITATION CHANGES

TO:

Approved for public release; distribution is unlimited.

FROM:

Distribution authorized to DoD only; Administrative/Operational Use; 15 JAN 1953. Other requests shall be referred to Office of the Chief of Ordnance, Department of the Army, Washington, DC 20310. Pre-dates formal DoD distribution statements. Treat as DoD only.

AUTHORITY

USAMC ltr dtd 26 Mar 1981; USAMC ltr dtd 26 Mar 1981

THIS REPORT HAS BEEN DECLASSIFIED
AND CLEARED FOR PUBLIC RELEASE.

<u>DISTRIBUTION A</u>
APPROVED FOR PUBLIC RELEASE;
DISTRIBUTION UNLIMITED.

CONFIDENTIAL
Security Information

NORTH AMERICAN INSTRUMENTS INC.

LOKI

WIND RESPONSE

ANALYSIS

by

Donald L. Baker
and
Warren L. Phillips

Design and Development of a Wind Correction Computer
For Use with M33 Director
in the Fire Control for LOKI Rockets

January 15, 1953

This Report supersedes the Supplementary Quarterly Report
dated October 31, 1952

CONFIDENTIAL
Security Information

ACKNOWLEDGMENT

TABLE OF CONTENTS

ILLUSTRATIONS

INTRODUCTION

The purpose of the present analysis is to determine the effect of an arbitrary wind distribution upon the trajectory of the LOKI missile. The parameters are presented in a fashion to facilitate the design of a computer to correct for wind. Further, the parameters are adaptable to correcting for varying winds which may exist during the missile's flight. The effect of winds is treated to rocket burnout only. The problem is treated in two parts; i.e., the calculation of sideways momentum and angular momentum inparted by a unit wind impulse, and step-by-step calculation of the resulting flight path deviation due to the impulse.

A drawing of the LOKI is shown in Figure 1 and the performance characteristics are given in Table I.

ANALYSIS

The LOKI missile rotates at a speed of approximately 100 radians per second. As a result there arises the so-called Magnus effect which produces (1) a circulation around the missile and a resulting lift force and (2) gyroscopic moments due to rotation. Both of these terms have been neglected in the present analysis on the basis of a careful study previously carried out by Dr. J. E. Froehlich of the California Institute of Technology Jet Propulsion Laboratory. Dr. Froehlich reported that he had included these effects in some exact LOKI

-2-

trajectory calculations involving a constant wind and found their contribution

to be negligible. In the present analysis it is further assumed that the effect

of thrust malalignment upon the trajectory may be treated as a separate phenom-

enon, and thus may be neglected here. The wind is treated as a perturbation

on the trajectory with no wind.

The general equations of motion in one plane and a figure for the geometri-

cal relationships are as follows:
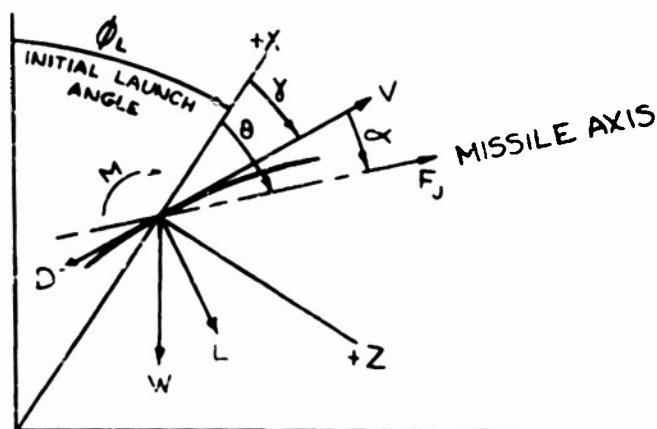
$$\sum F_{\text{ALONG FLIGHT PATH}} = 0$$

$$F_J \cos\alpha - D - W\cos(\phi_L + \gamma) - m\dot{V} = 0 \tag{1}$$

$$\sum F_{\perp \text{ FLIGHT PATH}} = 0$$

$$L_\alpha \cdot \alpha + F_J \sin\alpha + W\sin(\phi_L + \gamma) - mV\dot{\gamma} = 0 \tag{2}$$

$$\sum M = 0 \tag{3}$$

$$I\ddot{\theta} - M_{\dot{\theta}} \cdot \dot{\theta} - M_\alpha \cdot \alpha = 0$$

The velocity V, along the flight path has been obtained from Reference A for
the case of no wind. It is assumed in this analysis that the forward speed
will not be altered appreciably by winds because of the high forward acceler-
ation (approximately 125 g's initially and 250 g's at end of burning) and high
speed. There is, therefore, no need for including equation (1) in this analy-
sis and it has been dropped. It is to be noted that the third term of equation
(2) causes flight path curvature due to gravity. This effect is accounted for
in the trajectory without wind and thus may be neglected in this wind pertur-
bation analysis. A definition of terms in equations (2) and (3) is included in
Appendix A, the jet damping derivative in Appendix B and the aerodynamic
damping in Appendix C.

Rewriting equations (2) and (3) using $\alpha = \theta - \gamma$ and setting $\cos \gamma = 1.0$,
$\sin \gamma = \gamma$ and $\sin \alpha = \alpha$ because these angles are small, we find

$$\dot{\gamma} = \left[\frac{L_\alpha + F_J}{m V} \right] (\theta - \gamma) \tag{2a}$$

$$\ddot{\theta} = \left[\frac{M_{J\dot{\theta}} + M_{A\dot{\theta}}}{I} \right] \dot{\theta} + \frac{M_\alpha}{I} (\theta - \gamma) \tag{3a}$$

Thus far, the effect of wind has not been taken into account in the equation
of motion. The wind may be taken as an increment in angle of attack, $\Delta\alpha = \frac{w}{V}$
where w is the wind velocity component (feet/second) normal to the flight

path and in the plane under consideration. The flight path angle, γ , during booster rocket burning changes less than two degrees so the wind may be broken up into its three components with respect to the launching direction, w_x, w_y, and w_z. The effect of w_x (the component along the flight path) is negligible as stated previously. The effect of w_y and w_z are considered independent and are treated separately.

We now write equations (2a) and (3a) with the wind as a forcing function,

$$\dot{\gamma} - \left[\frac{L_\alpha + F_J}{mV}\right](\theta - \gamma) = \frac{L_\alpha}{mV} \cdot \frac{w}{V} \qquad (2b)$$

$$\ddot{\theta} - \left[\frac{M_{J_\phi} + M_{A\dot{\theta}}}{I}\right]\dot{\theta} - \frac{M_\alpha}{I}(\theta - \gamma) = \frac{M_\alpha}{I} \cdot \frac{w}{V} \qquad (3b)$$

Integrating equation (2b) with respect to time, we get

$$(\gamma_{\Delta t} - \gamma_o) - \int_o^{\Delta t}\left[\frac{L_\alpha + F_J}{mV}\right](\theta - \gamma)\,dt = \int_o^{\Delta t}\frac{L_\alpha}{mV} \cdot \frac{w}{V}\,dt \qquad (4)$$

Now if we consider a wind blowing from time zero to Δt and if we let $\Delta t \longrightarrow 0$ while holding the product $w \cdot \Delta t = 1.0$ so that we have a unit wind impulse, we get, upon completing the integration,

$$\Delta\gamma_i(t) = (\gamma_{\Delta t} - \gamma_o) = \frac{L_\alpha}{mV} \cdot \frac{1}{V} \qquad (5)$$

-5-

$\Delta \gamma_i(t)$ then represents the immediate effect of the wind impulse upon γ.

Similarly we obtain

$$\Delta \dot{\theta}_i(t) = \frac{M_\alpha}{I} \cdot \frac{1}{V} \tag{6}$$

from equation (3b).

$\frac{L_\alpha}{mV} \cdot \frac{1}{V}$ and $\frac{M_\alpha}{I} \cdot \frac{1}{V}$ are considered constant in the above integrations be-

cause $\Delta t \longrightarrow 0$. It is to be noted that $\Delta \gamma_i(t)$ is independent of forward

velocity. This is shown by substituting

$$L_\alpha = \frac{1}{2} \rho V^2 b^2 \frac{dC_L}{d\alpha} \qquad \text{in equation (5)}$$

$$\Delta \gamma_i(t) = \frac{\frac{1}{2}\rho V^2 b^2 \frac{dC_L}{d\alpha}}{mV} \cdot \frac{1}{V}$$

$$\Delta \gamma_i(t) = \frac{\frac{1}{2}\rho b^2 \frac{dC_L}{d\alpha}}{m} \tag{7a}$$

$\Delta \dot{\theta}_i(t)$ increases as a function of V and is shown by substituting

$M_\alpha = \frac{1}{2}\rho V^2 b^3 C_{M_\alpha}$ in equation (6)

$$\Delta \dot{\theta}_i(t) = \frac{\frac{1}{2}\rho V^2 b^3 C_{M_\alpha}}{I} \cdot \frac{1}{V}$$

$$\Delta \dot{\theta}_i(t) = \frac{\frac{1}{2}\rho b^3 C_{M_\alpha}}{I} \cdot V \tag{7b}$$

Curves of $\Delta \gamma_i(t)$ and $\Delta \dot{\theta}_i(t)$ are shown in Figures 2 and 3. $\Delta \gamma_i(t)$ and

$\Delta \dot{\theta}_i(t)$ are then the increments developed immediately upon application of

the unit wind impulse. To determine the error at the end of rocket burning, an integration must be made recognizing the fact that the coefficients vary with time. Equations (2a) and (3a) were rewritten in the form

$$\dot{\gamma} = 2\lambda_1 (\theta - \gamma) \tag{8}$$

$$\ddot{\theta} = - \left[2\lambda_o \dot{\theta} + \omega_o^2 (\theta - \gamma) \right] \tag{9}$$

where

$$2\lambda_1 = \frac{L_\alpha + F_J}{mV}$$

$$2\lambda_o = - \left[\frac{M_{J\phi} + M_{A\dot{\theta}}}{I} \right]$$

and

$$\omega_o^2 = - \frac{M_\alpha}{I}$$

Using $\alpha = \theta - \gamma$, the simultaneous solution of equations (8) and (9) becomes

$$\ddot{\alpha} + 2(\lambda_1 + \lambda_o)\dot{\alpha} + (4\lambda_o\lambda_1 + 2\dot{\lambda}_1 + \omega_o^2)\alpha = 0 \tag{10}$$

then letting

$$\lambda_e = \lambda_1 + \lambda_o$$

and

$$\omega_e^2 = 4\lambda_o\lambda_1 + 2\dot{\lambda}_1 + \omega_o^2$$

equation (10) becomes

$$\ddot{\alpha} + 2\lambda_e\dot{\alpha} + \omega_e^2 \alpha = 0 \tag{11}$$

As a solution let

$$\alpha = e^{-\lambda_e t} \left\{ A\cos\omega t + B\sin\omega t \right\} \tag{12}$$

where

$$\omega = \sqrt{\omega_e^2 - \lambda_e^2}$$

From equation (12) we obtain

$$\dot{\alpha} = e^{-\lambda_e t} \left[-\lambda_e \{ A \cos \omega t + B \sin \omega t \} + \{ -A \omega \sin \omega t + B \omega \cos \omega t \} \right] \qquad (13)$$

From equations (12) and (13) we find at $t = 0$

$$\alpha_o = A$$

$$\dot{\alpha}_o = B\omega - \lambda_e A = B\omega - \lambda_e \alpha_o$$

$$B = \frac{\dot{\alpha}_o + \lambda_e \alpha_o}{\omega}$$

Thus equations (12 and (13 become

$$\alpha(t_1) = e^{-\lambda_e t_1} \left\{ \alpha_o \cos \omega t_1 + \left(\frac{\dot{\alpha}_o + \lambda_e \alpha_o}{\omega} \right) \sin \omega t_1 \right\} \qquad (14)$$

$$\dot{\alpha}(t_1) = e^{-\lambda_e t_1} \left[-\left\{ \alpha_o \frac{\omega_o^2}{\omega} + \dot{\alpha}_o \frac{\lambda_e}{\omega} \right\} \sin \omega t_1 + \dot{\alpha}_o \cos \omega t_1 \right] \qquad (15)$$

From equation (8)

$$\gamma(t_1) = \Delta\gamma_i + \int_o^{t_1} 2\lambda_1 \alpha \, dt = \Delta\gamma_i + \sum_o^{t_1} 2\lambda_1 \alpha \cdot \Delta t \qquad (16)$$

A sample step-by-step calculation using the above method was run for a gust occurring at .3 of a second after initiation of burning. This was run as a check point on the work done by Dr. Froehlich and is shown in Appendix D. This check agreed with Dr. Froehlich's calculations within five percent.

An attempt to compute the trajectory step-by-step using a linear extrapolation over the time interval proved to be unsatisfactory, due to the very high accelerations. The above described sinusoidal extrapolation was more laborious but gave satisfactory accuracy with manual computation.

of $2\lambda_1$, $2\lambda_e$, and ω_1^2 are given in Figs. 4, 5, and 6 and in Table II.

The final values of flight path deviation at fuel burnout $\Delta\gamma_F(t)$ due to the wind impulses are shown in Fig. 7 plotted versus time. (The values for this curve were determined from work done by Dr. Froehlich.) This term $\Delta\gamma_F(t)$ which we shall call the influence coefficient, is then the integrated effect of a unit crosswind impulse applied at a particular time.

The total flight path angular deviation, $\Delta\gamma_T$, due to a continuous distribution of winds may be calculated by integrating the product of the influence coefficient and the crosswind in feet per second from zero to the time at the end of the boost, the equation being

$$\Delta\gamma_T = \int_0^{t_1} \left[\Delta\gamma_F(t) \cdot w(t) \right] dt \qquad (17)$$

where $\Delta\gamma_F(t)$ and $w(t)$ are the values of the influence coefficient and the wind at the time under consideration.

It is to be remembered that the value of γ given by equation (16) is the direction of the flight path of the center of gravity of the complete LOKI. The direction of the c.g. of the DART (the forward body) differs from this because of the distance between these two c.g.'s if there is a residual $\dot\theta$. γ_F does not completely define the eventual direction of the DART, $\dot\alpha$ and $\dot\gamma$ are also boundary conditions. Because of lack of data, it is not possible to evaluate these two additional effects, however, when data becomes available an evaluation of them will be made. They will be most effective, of course, when gusts occur late in the boost phase.

-9-

To facilitate the determination of the error due to wind when the wind is known as a function of distance along the flight path instead of in terms of time, we shall use a wind impulse defined as $w \cdot \Delta s = 1.0$. On this basis we may show equations (2b) and (3b) as

$$\int \dot{\gamma} \, dt \cdot \frac{ds}{dt} - \int \left[\frac{L_\alpha + F_J}{mV}\right](\theta - \gamma) \, dt \cdot \frac{ds}{dt} = \int \frac{L_\alpha}{V} \cdot \frac{w}{V} \, ds$$

$$\int \ddot{\theta} \, dt \cdot \frac{ds}{dt} - \int \left[\frac{M_{J\dot\theta} + M_{A\dot\theta}}{I}\right]\dot{\theta} \, dt \cdot \frac{ds}{dt} - \int \frac{M_\alpha}{I}(\theta - \gamma) \, dt \cdot \frac{ds}{dt} = \int \frac{M_\alpha}{I} \cdot \frac{w}{V} \cdot ds$$

however $\frac{ds}{dt} = V$, so

$$\int \dot{\gamma} \, dt - \int \frac{L_\alpha + F_J}{mV}(\theta - \gamma) \, dt = \int \frac{L_\alpha}{mV} \cdot \frac{1}{V} \cdot \frac{w}{V} \, ds$$

$$\int \ddot{\theta} \, dt - \int \left[\frac{M_{J\dot\theta} + M_{A\dot\theta}}{I}\right] \dot{\theta} \, dt - \int \frac{M_\alpha}{I}(\theta - \gamma) \, dt = \int \frac{M_\alpha}{I} \cdot \frac{1}{V} \cdot \frac{w}{V} \, ds$$

Now integrating as we did to get equations (5) and (6) and substituting for $w \cdot \Delta s = 1.0$, we get

$$\Delta \gamma_i(s) = \frac{L_\alpha}{mV} \cdot \frac{1}{V^2} \tag{18}$$

$$\Delta \dot{\theta}_i(s) = \frac{M_\alpha}{I} \cdot \frac{1}{V^2} \tag{19}$$

It is seen that $\Delta \gamma_i(s) = \Delta \gamma_i(t) \cdot \frac{1}{V}$ and $\Delta \dot{\theta}_i(s) = \Delta \dot{\theta}_i(t) \cdot \frac{1}{V}$ so that $\Delta \gamma_i(s)$ decreases as a function of V and $\Delta \dot{\theta}_i(s)$ is independent of V.

-10-

Curves of $\Delta\gamma_i(s)$ and $\Delta\dot{\theta}_i(s)$ are shown as Figs. (8) and (9). The sharp peak (negative) in $\Delta\dot{\theta}_i(s)$ at 180 feet is due mainly to the relatively high static stability margin at this point. The static margin is approximately three times as high at this point as at other points in the trajectory. The rise in $\Delta\dot{\theta}_i(s)$ towards the end of burning is due to the decreasing moment of inertia. Fig. 10 shows the influence coefficient, $\Delta\gamma_F(s)$, as a function of distance where

$$\Delta\gamma_F(s) = \frac{1}{V} \cdot \Delta\gamma_F(t).$$

The total flight path angular deviation due to winds may thus be obtained by

$$\Delta\gamma_T = \int_0^s \left[\Delta\gamma_F(s) \cdot W(s)\right] ds \qquad (20)$$

or by use of equation (19).

TABLE I

LOKI PERFORMANCE CHARACTERISTICS

Initial weight of booster plus Dart = 24.30 lbs.

Final weight of booster plus Dart = 12.23 lbs.

Weight of booster propellant = 12.07 lbs.

Weight of Dart only = 6.3 lbs.

CHARACTERISTICS AS A FUNCTION OF TIME				
Time, Seconds	Thrust, Pounds	I_{CG}	Mass $m = w/g$	Velocity Ft/sec
0	0	4.14	.756	0
.10	3120	4.00	.718	365
.20	3200	3.84	.673	825
.30	3275	3.65	.627	1300
.40	3300	3.45	.580	1830
.50	3325	3.24	.534	2400
.60	3300	2.99	.487	3025
.70	3160	2.74	.440	3690
.80	2125	2.49	.400	4260
.90	520	2.36	.382	4475

TABLE II

STABILITY AND FLIGHT PATH CHARACTERISTICS

Time, Seconds	$M_{\dot{e}}/I$	$M_{A_{\dot{e}}}/I$	$M_{\alpha}/I = -\omega_o^2$	$\dfrac{M_{J_{\dot{e}}}+M_{A_{\dot{e}}}}{I} = -2\lambda_o$	$\dfrac{F_J+L_\alpha}{mV} = 2\lambda_1$	λ_o	ω_o
0	-1.15	0	.0	-1.15	∞	.575	.0
.05	-1.20	- .0915	- 1.056	-1.292	27.519	.646	1.030
.10	-1.25	- .272	- 6.76	-1.522	12.08	.761	2.60
.15	-1.275	- .437	- 18.4	-1.712	8.01	.856	4.290
.20	-1.315	- .650	- 40.8	-1.965	6.19	.9825	6.36
.25	-1.365	- .950	- 108.0	-2.315	5.30	1.157	10.40
.30	-1.44	-1.28	- 234.0	-2.72	4.84	1.330	15.28
.35	-1.50	-1.45	- 302.0	-2.95	4.51	1.475	17.40
.40	-1.60	-1.71	- 348.0	-3.31	4.28	1.655	18.66
.45	-1.68	-2.137	- 404.0	-3.817	4.22	1.908	20.16
.50	-1.80	-2.50	- 441.6	-4.30	4.25	2.150	21.04
.55	-1.92	-2.89	- 480.4	-4.81	4.37	2.405	21.96
.60	-2.07	-3.34	- 553.2	-5.41	4.48	2.705	23.52
.65	-2.23	-3.79	- 671.2	-6.02	4.81	3.01	25.96
.70	-2.40	-4.25	- 802.8	-6.65	4.89	3.325	28.32
.75	-2.60	-4.74	-1020.4	-7.34	5.01	3.67	31.98
.80	-2.84	-5.27	-1234.0	-8.11	4.83	4.055	35.10
.85	-3.00	-5.82	-1474.0	-8.82	4.49	4.410	38.40
.90	-3.08	-6.40	-1692.0	-9.48	4.35	4.74	41.10

TABLE III

INFLUENCE COEFFICIENTS $\Delta \gamma_F (t)$ and $\Delta \gamma_F (S)$

$$\Delta \gamma_F (S) = \Delta \gamma_F (t) \cdot \frac{1}{V}$$

$w \cdot \Delta t = 1.0$ at Time, sec.	$\Delta \gamma_F (t)$ Radians	V Ft/Sec	$\Delta \gamma_F (S) \times 10^3$ Radians	S Dist., Ft.
0	0	0	∞	0
.05	-0.56	150	-3.70	5
.1	-1.04	365	-2.85	15
.2	-1.05	825	-1.27	74
.3	-2.31	1300	-1.78	179
.4	-1.30	1830	-0.71	337
.5	-1.01	2400	-0.42	547
.6	-0.91	3025	-0.30	818
.7	-0.18	3690	-0.05	1154
.8	-0.64	4260	-0.15	1553
.9	+0.76	4475	+0.17	1993

APPENDIX A

LIST OF SYMBOLS

$$L_\alpha = \frac{dL}{d\alpha} = \frac{1}{2}\rho V^2 b^2 \cdot \frac{dC_L}{d\alpha}$$, slope of the lift curve in pounds per radian

$\rho = .00230$ air density in slugs/cu/ft.

V = forward velocity, ft/sec

b = diameter of booster body, ($b = .25$ ft)

$\frac{dC_L}{d\alpha}$ = slope of lift coefficient curve (assumed equal to $\frac{dC_N}{d\alpha}$ from

Reference (A), the slope of the normal force coefficient curve) per radian

α = angle of attack of missile body axis, radians

F_J = rocket jet thrust, pounds (obtained from Reference A)

W = instantaneous weight of missile, pounds

γ = angle between vertical and tangent to flight path, radians

m = instantaneous mass of the missile, slugs (obtained from Reference A)

$\dot{\gamma} = \frac{d\gamma}{dt}$ = radians per second

$I = I_{c.g.}$ = instantaneous moment of inertia of the missile about the Y axis,

slug-ft^2 $\left(m \times (K_1)^2 = I_{c.g.}, K_1^2 \text{ obtained from Reference A}\right)$.

APPENDIX A (contd)

LIST OF SYMBOLS

$$\ddot{\theta} = \frac{d^2\theta}{dt^2} = \text{radians /sec}^2$$

$$M_{\dot{\theta}} = \frac{\partial M}{\partial \dot{\theta}} = \frac{\partial M_J}{\partial \dot{\theta}} + \frac{\partial M_A}{\partial \dot{\theta}} = M_{J\dot{\theta}} + M_{A\dot{\theta}}$$

$M_{J\dot{\theta}}$ = rotational damping due to rocket jet. The derivation of this term is

    shown in Appendix C.

$M_{A\dot{\theta}}$ = rotational aerodynamic damping. Derivation shown in Appendix C.

$$M_\alpha = \frac{\partial M}{\partial \alpha} = \frac{1}{2} \rho V^2 b^3 C_{M_\alpha}$$

l_{CG} = distance from aft end of booster to instantaneous center of gravity,

    calibers (obtained from Reference A)

l_{CP} = distance from aft end of booster to instantaneous center of pressure,

    calibers (d x l_p from Reference A)

$$C_{M_\alpha} = (l_{CP} - l_{CG}) \frac{dC_N}{d\alpha}$$

$$\theta = \gamma + \alpha$$

APPENDIX B

JET DAMPING MOMENT

The effect of rocket jet damping due to angular missile velocity was obtained from Reference (b). The jet damping term of equation (3) from this reference is:

$$2 \sum^{j} m_i r v = M_{J_{\dot{\theta}}}$$

where $Q = \dot{\theta}$ = missile airframe angular velocity - radians/sec

m_i = incremental mass of gases at any section

r = distance of particle of gas under consideration from cg - ft.

v = velocity (ft/sec) of gas particle under consideration with respect to missile

Now $\rho_j A v$ = c, where

c = mass flow in slugs per sec. at a particular station

A = cross sectional area at section under consideration ft^2

ρ_j = mass density, $\dfrac{\#}{ft^3} \quad \dfrac{sec^2}{ft}$

v = $\dfrac{c}{\rho_j A}$

m_i = $\rho_j A \Delta r$

$$M_{J_{\dot{\theta}}} = 2 \sum^{j} m_i r v = \int \rho_j A dr \cdot r \frac{c}{\rho_j A} = 2 \int c r \, dr$$

APPENDIX B (Contd)

JET DAMPING MOMENT

Assuming equal rate of burning all along booster and neglecting nozzle length a plot of "c" would be:
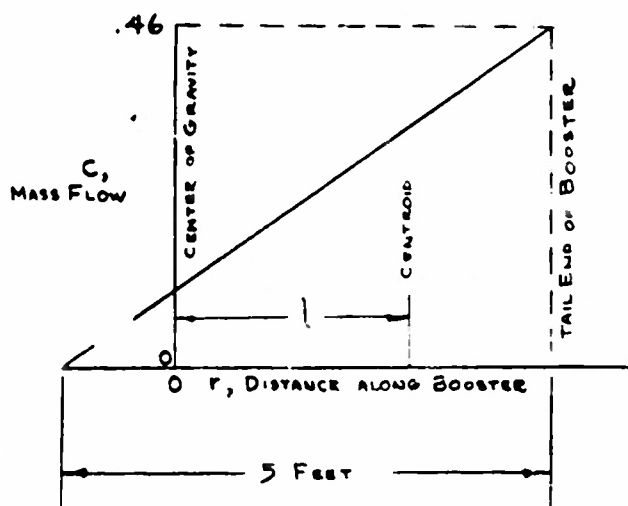
and $\int c\, dr = \dfrac{5 \times .46}{2} = 1.15.$ The integral of $Cr\, dr$ thus equals 1.15 l.

The distance of the centroid of $\int C\, dr$ from the tail end of the booster $=$

$1/3 \times 5$ ft. $= 1.667$ ft.

APPENDIX B (Contd)

JET DAMPING MOMENT

(1) Time	(2) Dist. from CG to Tail End of Booster, feet	(3) l, Feet $=(2)-1.667$	(4) $\sum m_i r v = \int c r d r = 1.15 \times (3)$	(5) $\sum m_i r v = (2) \times (4) = M_{j\dot\theta}$	(6) I_{CG}	(7) $\dfrac{M_{j\dot\theta}}{I}$
0	3.75	2.08	2.39	4.78	4.14	1.154
.1	3.80	2.13	2.45	4.90	4.00	1.25
.2	3.87	2.20	2.53	5.06	3.84	1.319
.3	3.97	2.30	2.64	5.28	3.65	1.445
.4	4.07	2.40	2.76	5.52	3.45	1.60
.5	4.20	2.53	2.91	5.82	2.24	1.798
.6	4.35	2.68	3.08	6.16	2.99	2.06
.7	4.54	2.87	3.30	6.60	2.74	2.41
.8	4.73	3.06	3.52	7.04	2.49	2.83
.9	4.83	3.16	3.63	7.26	2.36	3.08

APPENDIX C

AERODYNAMIC DAMPING IN PITCH

The damping moment derivative which is denoted by $M_{A\dot{\theta}}$ is obtained in the following manner:

Consider the missile to have a lifting surface i located at a distance x_i from the c.g.
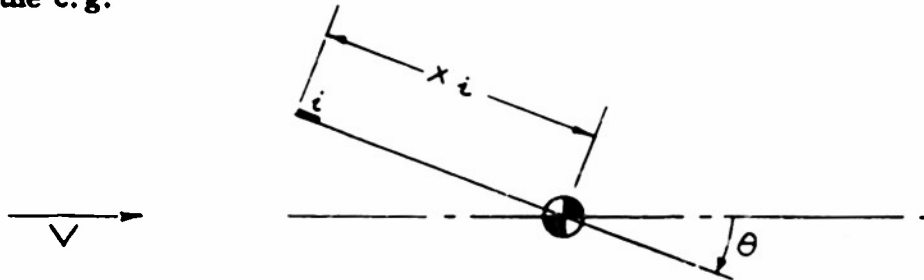
This surface will experience an induced angle of attack equal to $\dfrac{x_i \dot{\theta}}{V}$ due to the angular velocity $\dot{\theta}$ in pitch. The Moment $M_i = \left(\dfrac{dC_N}{d\alpha}\right)_i \cdot \dfrac{q S x_i^2 \dot{\theta}}{V}$ acts in a direction opposite to that of $\dot{\theta}$. The total moment is obtained by summing over all the lifting surfaces.

$$M = \sum M_i = \frac{q S \dot{\theta}}{V} \sum_{i=1}^{n} \left(\frac{dC_N}{d\alpha}\right)_i \cdot x_i^2$$

The damping moment derivative which is obtained by differentiating the above expression with respect to $\dot{\theta}$ is

$$M_{\dot{\alpha}} = \frac{q S}{V} \sum_{i=1}^{n} \left(\frac{dC_N}{d\alpha}\right)_i \cdot x_i^2$$

SAMPLE STEP-BY-STEP CALCULATION

REFERENCES

Reference   (A) Letter dated 19 August 1952 from Louis G. Dunn, Jet Propulsion Laboratory, California Institute of Technology, to Bernard Helfand, North American Instruments, Inc.

(B) Barton, M. V., The Effect of Variation of Mass on the Dynamic Stability of Jet-Propelled Missiles, Journal of Aeronautical Sciences, April 19⁵0.
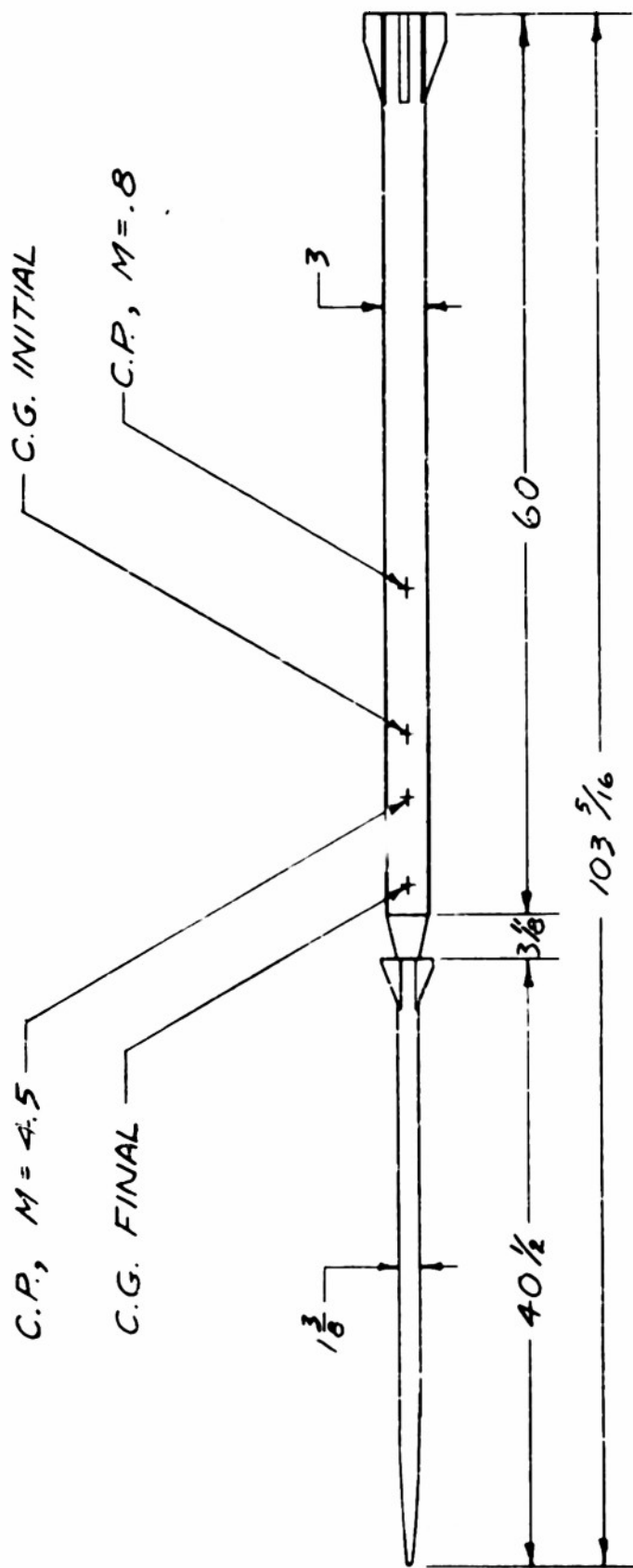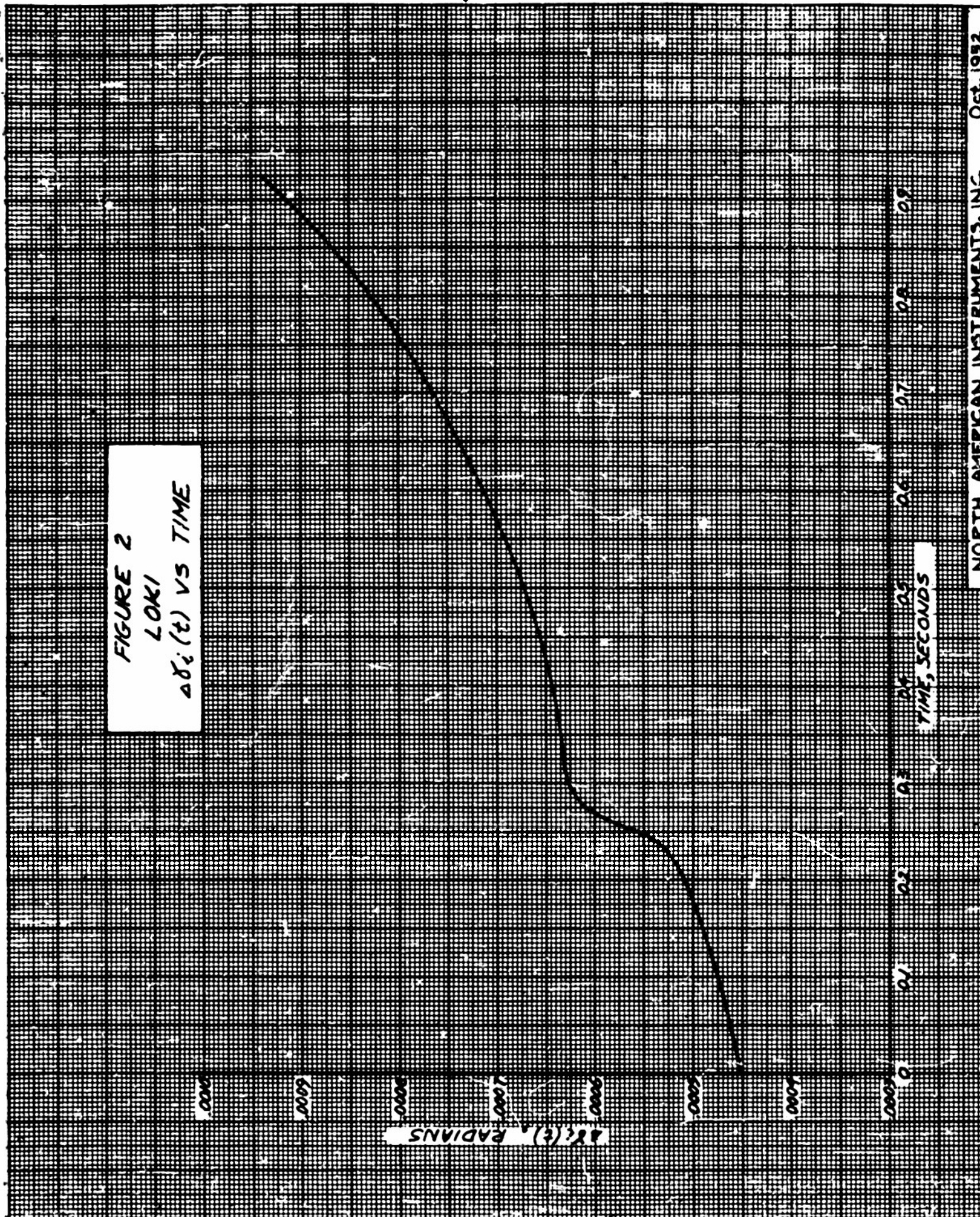
FIGURE 1
LOKI

NORTH AMERICAN INSTRUMENTS, INC.   Oct. 1952

FIGURE 2
LOKI
$\Delta \delta_i(t)$ VS TIME

NORTH AMERICAN INSTRUMENTS, INC.   Oct, 1952
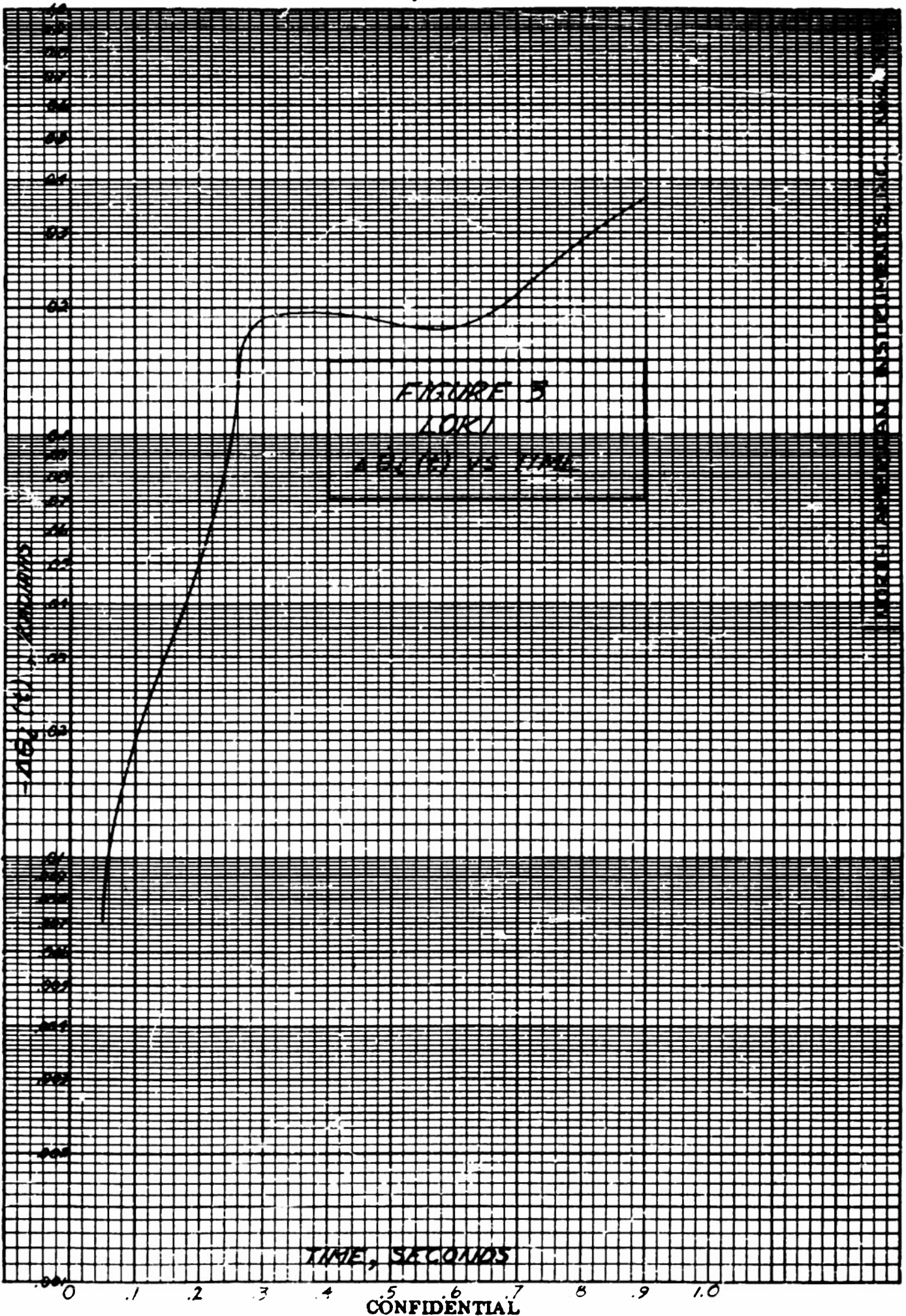
FIGURE 5
LOKI
ARs (r) vs TIME

TIME, SECONDS

FIGURE 4
LOKI
ΣA_i VS TIME
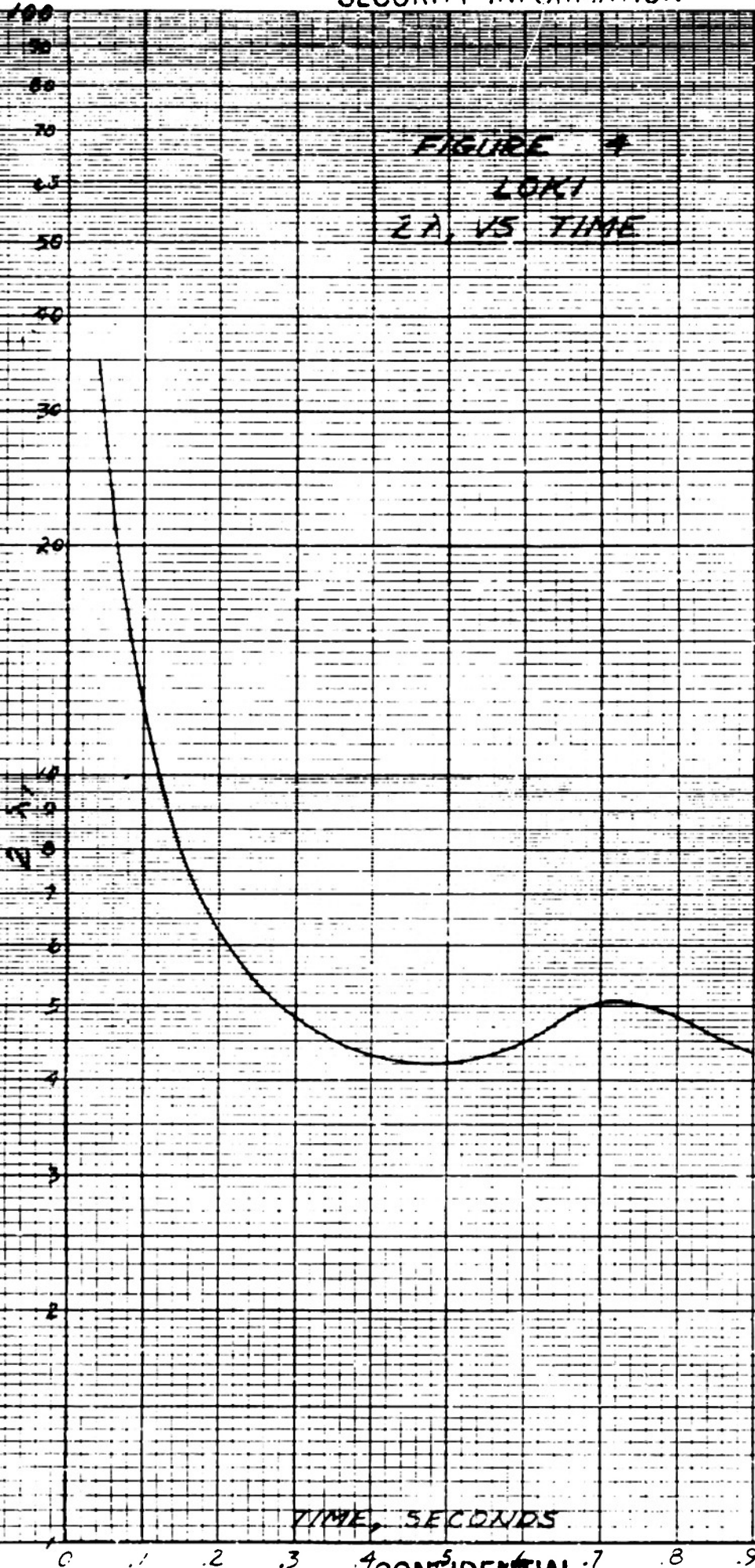
TIME, SECONDS

FIGURE 5
LOKI
C.A. VS TIME

TIME, SECONDS

FIGURE 8
LGM
ω_e^2 vs TIME

TIME, SECONDS
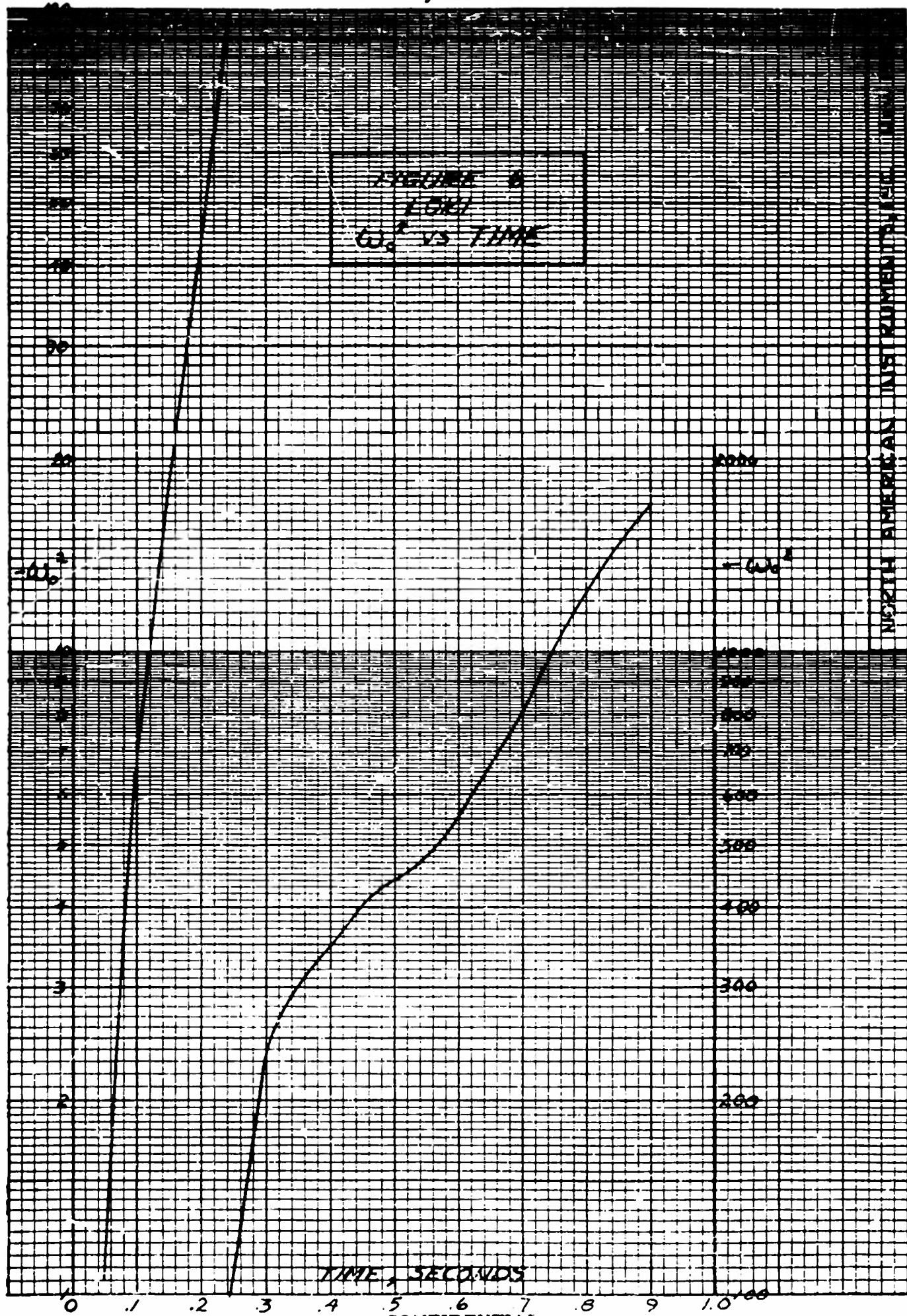
FIGURE 7
LOKI
INFLUENCE COEFFICIENT, $\delta_{F}(t)$

NORTH AMERICAN INSTRUMENTS, INC.   Dec. 1922
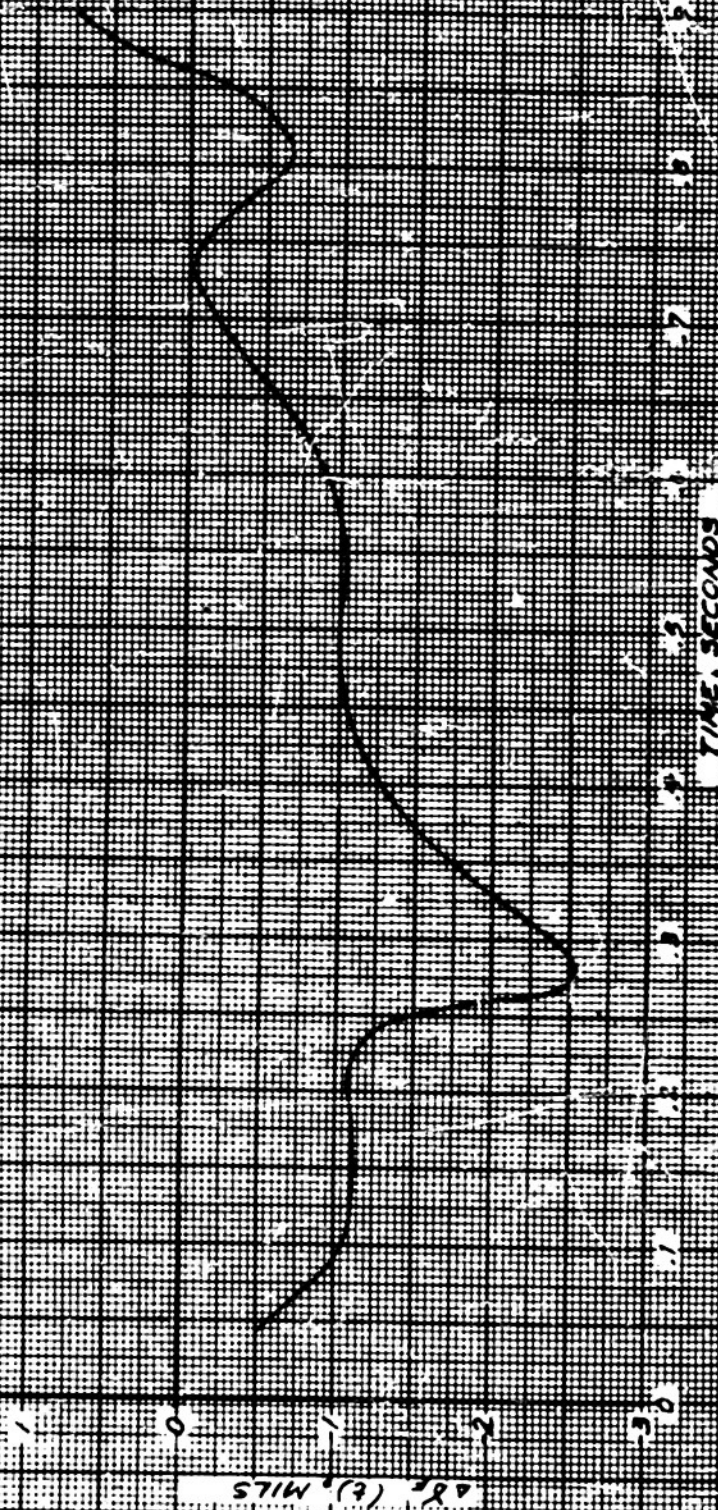
FIGURE 8
LOKI
$\Delta \dot{\gamma}_i(s)$ VS DISTANCE

NORTH AMERICAN INSTRUMENTS, INC.   Oct. 1952

FIGURE 9
LOKI
$\Delta\dot{\theta}_i(s)$ vs DISTANCE

FIGURE 10
LOKI
INFLUENCE COEFFICIENT, δʳₓ (s)